



Comparative examination of the pons and corpus callosum as reference regions for quantitative evaluation in positron emission tomography imaging for Alzheimer's disease using ¹¹C-Pittsburgh Compound-B

Tomohiro Tada¹ · Kazuhiro Hara² · Naotoshi Fujita¹ · Yoshinori Ito³ · Hiroshi Yamaguchi⁴ · Reiko Ohdake⁵ · Kazuya Kawabata^{2,6} · Aya Ogura² · Toshiyasu Kato^{2,7} · Takamasa Yokoi⁸ · Michihito Masuda^{2,9} · Shinji Abe¹ · Shinichi Miyao¹⁰ · Shinji Naganawa¹¹ · Masahisa Katsuno^{2,12} · Hirohisa Watanabe⁵ · Gen Sobue¹³ · Katsuhiko Kato¹⁴

Received: 18 December 2022 / Accepted: 24 April 2023 / Published online: 9 May 2023
© The Author(s) 2023

Abstract

Objectives Standardised uptake value ratio (SUVR) is usually obtained by dividing the SUV of the region of interest (ROI) by that of the cerebellar cortex. Cerebellar cortex is not a valid reference in cases where amyloid β deposition or lesions are present. Only few studies have evaluated the use of other regions as references. We compared the validity of the pons and corpus callosum as reference regions for the quantitative evaluation of brain positron emission tomography (PET) using ¹¹C-PiB compared to the cerebellar cortex.

Methods We retrospectively evaluated data from 86 subjects with or without Alzheimer's disease (AD). All subjects underwent magnetic resonance imaging, PET imaging, and cognitive function testing. For the quantitative analysis, three-dimensional ROIs were automatically placed, and SUV and SUVR were obtained. We compared these values between AD and healthy control (HC) groups.

Results SUVR data obtained using the pons and corpus callosum as reference regions strongly correlated with that using the cerebellar cortex. The sensitivity and specificity were high when either the pons or corpus callosum was used as the reference region. However, the SUV values of the corpus callosum were different between AD and HC ($p < 0.01$).

Conclusions Our data suggest that the pons and corpus callosum might be valid reference regions.

Keywords Standardised uptake value ratio · Brain · Positron emission tomography imaging · ¹¹C-Pittsburgh Compound-B · Alzheimer's disease

Introduction

Alzheimer's disease (AD) is pathologically characterised by neurofibrillary tangles and amyloid β (A β) deposition. A β deposition is a pathological feature that arises from the earliest stages of AD onset and begins decades before the onset of cognitive decline [1]. ¹¹C-Pittsburgh compound-B (PiB) is an amyloid imaging agent developed by Mathis et al., derived from the structure of thioflavin T, which is used to detect A β deposition in vitro [2]. Amyloid imaging

with ¹¹C-PiB enables the visualisation of A β deposition in the brain. Amyloid imaging has made it possible to evaluate A β deposition in the brain before death; however, it still has to be confirmed at autopsy [3]. Therefore, amyloid imaging using positron emission tomography (PET) is important for the early diagnosis of AD. The development of therapeutic agents for AD has been a focal area of research [4, 5]. Besides helping in AD diagnosis, amyloid imaging with ¹¹C-PiB PET also aids in evaluating the therapeutic effect of clinical treatments. Several studies have used the standardised uptake value ratio (SUVR) as a quantitative evaluation of brain PET using ¹¹C-PiB [3, 6, 7]. SUVR is obtained by dividing the SUV of the region of interest (ROI) by that of the reference region. Generally, SUVR is evaluated using the

✉ Katsuhiko Kato
katokt@med.nagoya-u.ac.jp

Extended author information available on the last page of the article

cerebellar cortex as the reference region. However, significant amyloid deposition has been reported in the cerebellar cortex of familial AD and in severe AD cases [6]. Furthermore, some patients with cerebral amyloid angiopathy or a certain type of systemic amyloidosis also have significant amyloid deposition in the cerebellum [8, 9]. Moreover, some elderly people have cerebellar disorders, such as cerebellar haemorrhage or cerebellar infarction. Cerebellar infarction accounts for 2–4% of ischaemic strokes, and cerebellar haemorrhage accounts for approximately 10% of all cerebral haemorrhages and, therefore, is not considered a rare disease [10–12]. In these cases, the cerebellar cortex may not be available to use as a reference region. Therefore, few studies have evaluated the pons and the white matter as reference areas [7, 13]. Moreover, the study examined only a small number of subjects or used complicated methods. Thus, in order to improve the generalisability of the conclusions, there is a need for a larger number of study subjects and a less complicated analysis.

In this study, we compared the validity of the pons and corpus callosum as reference regions for the quantitative evaluation of brain PET using ^{11}C -PiB with reference to the cerebellar cortex as a reference region. For the initial investigation, we used general AD patients and healthy controls (HCs).

Materials and methods

Subjects

In this study, we retrospectively evaluated the data of 86 subjects (23 AD patients and 63 HCs). All subjects underwent magnetic resonance imaging (MRI), PET imaging with ^{11}C -PiB, and cognitive function assessments, which included the Mini-Mental State Examination (MMSE) [14], Addenbrooke's Cognitive Examination Revised (ACE-R) [15], AD Assessment Scale-Cognitive-Japanese (ADAS-cog-j) [16], Logical Memory II of the Wechsler Memory Scale Revised [17], Clinical Dementia Rating (CDR) [18], and CDR Scale Sum of Boxes (CDR-SB) [19].

All AD patients were recruited from the outpatient clinic of our hospital and the Department of Meitetsu Hospital in Nagoya. HCs were recruited from a healthy cohort of an ageing study at our research centre. We defined AD and HCs based on the criteria of Yokoi et al. [20]. In their report, the criteria for diagnosis of AD were as follows: (1) memory complaint; (2) 0.5 or 1.0 in CDR; (3) a score lower than one standard deviation (SD) minus the average of their ages in Logical Memory II; and (4) PiB positive. They assessed the

patients as "PiB positive" if the SUVRs, calculated with the cerebellar cortex as a reference region, was larger than 1.5. Clinical diagnoses were made based on the consensus of the three neurologists. This study was approved by the research ethics committee of our hospital (2020-0412, 2019-0033).

^{11}C -PiB PET imaging

^{11}C -PiB PET imaging was obtained at our hospital and performed between 50 and 70 min after an intravenous injection of 555 MBq of ^{11}C -PiB. PET imaging was performed using a Biograph16 (Siemens Healthineers, Erlangen, Germany) in the three-dimensional scanning mode, 256×256 matrix, and an acquisition time of 20 min. All imaging data were reconstructed by Fourier rebinning and an ordered subset expectation maximisation algorithm, with a combination of numbers of the subset 16 and iteration 2 and a 5 mm Gaussian post-filter using syngo VB40B (Siemens Healthineers, Germany). All imaging data were reconstructed following computed tomography-based attenuation correction and single scatter simulation.

MR imaging

All MRI scans were performed using MAGNETOM Verio 3 T (Siemens Healthineers, Erlangen, Germany), 32-channel head matrix coil (Siemens Healthineers, Erlangen, Germany) at our research centre. T1-weighted volumetric MR images (repetition time = 2.5 s, echo time = 2.48 ms, flip angle = 8° , field of view = $256 \times 256 \times 192$ voxels, voxel size = $1 \times 1 \times 1$ mm, band width = 170 Hz/pixel, acquisition time = 353 s) were acquired for co-registration with the PET images.

Image analysis

We used PMOD software (version 3.9; PMOD Technologies, Zurich, Switzerland) and the PNEURO tool for the quantitative analysis of ^{11}C -PiB PET images. Three-dimensional ROIs were automatically placed, and the SUVR of each ROI was obtained using the following method: The T1-weighted volumetric MR images were automatically segmented into gray matter, white matter, and cerebrospinal fluid. ^{11}C -PiB PET and segmented MR images for each subject were co-registered, and the MR images were spatially normalised into the standard Montreal Neurological Institute T1 template. The transformation parameters of the normalised MR images were applied to the corresponding PET images. The Hammers N30R83 maximum probability atlas was adapted to the MR images of each subject. ROI information was

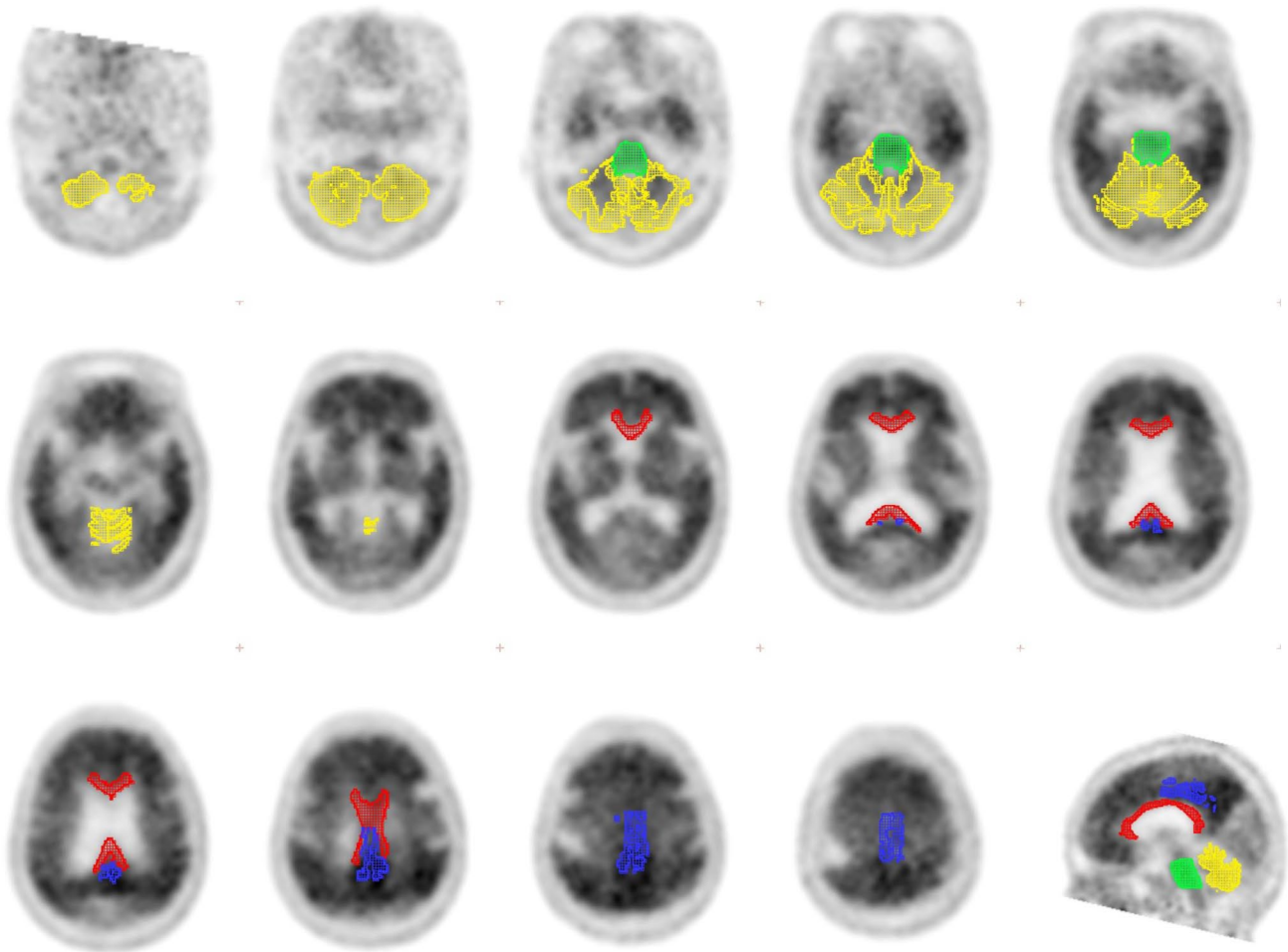


Fig. 1 The ROIs of the reference regions. Cerebellar cortex (yellow), pons (green), and corpus callosum (red), posterior cingulate cortex (blue)

applied to the PET images of the subject [21, 22]. Figure 1 shows the results of ROIs adapted in the MR images.

It is known that A β deposits in the posterior cingulate cortex during the early stages of AD onset [23, 24]. Therefore, SUVR was calculated using the SUVmean of the posterior cingulate cortex as the ROI, and the cerebellar cortex, pons, and corpus callosum as the reference regions. These SUVRs are defined as SUVR_cerebellar cortex, SUVR_pons, and SUVR_corpus callosum.

Statistical analysis

The results are expressed as mean \pm SD. Clinical backgrounds were compared using a non-parametric test (Mann–Whitney U test or chi-squared test). We examined correlations between SUVR_cerebellar cortex, SUVR_pons, and SUVR_corpus callosum using Spearman's rank correlation coefficient. In addition, the Bland–Altman analysis

was performed for comparison between SUVR_cerebellar cortex and both SUVR_pons and SUVR_corpus callosum. We used the Statistical Package for the Social Sciences software (Version 27; SPSS Inc., Chicago, IL, USA) for statistical analyses. We investigated the relationship between SUVR_cerebellar cortex in the posterior cingulate cortex and SUVR_pons/SUVR_cerebellar cortex and SUVR_corpus callosum/SUVR_cerebellar cortex. Receiver operating characteristic (ROC) analysis was used to evaluate the sensitivity and specificity of SUVR determined using the cerebellar cortex, pons, and corpus callosum as reference regions. The cut-off values were also calculated. ROC analysis was performed using the statistical software R (version 4.1.3). The SUV mean of pons and corpus callosum were compared between AD and HC. We used the Mann–Whitney U test in the Statistical Package for the Social Sciences software for statistical analyses. The threshold for statistical significance was set at $p < 0.01$.

Table 1 Patient characteristics

	Healthy control (HC)	Alzheimer's disease (AD)	p-value
Number	63	23	N.A
Age at examination	67.4±8.3	68.6±7.6	N.S. ^a
Male:female	22:41	4:19	N.S. ^b
Education (year) ¹	13.9±2.4	13.4±1.8	N.S. ^a
CDR ²	0.0±0.0	0.67±0.24	<0.001 ^a
CDR-SB ³	0.0±0.0	2.9±1.1	<0.001 ^a
MMSE ⁴	29.3±1.2	23.6±2.7	<0.001 ^a
ADAS-cog-j ⁵	3.4±1.7	12.6±5.2	<0.001 ^a
Logical memory II ⁶	19.6±6.1	1.0±1.7	<0.001 ^a
ACE-R ⁷	97.8±2.4	75.1±8.8	<0.001 ^a

Data are shown as mean±standard deviation. ^aHC vs. AD using the Mann–Whitney U test, ^bHC vs. AD using the chi-square test. N.S. not significant, N.A. not applicable

¹Education: Years of school

²CDR: Clinical Dementia Rating

³CDR-SB: CDR Scale Sum of Boxes

⁴MMSE: Mini Mental State Examination

⁵ADAS-cog-j: AD Assessment Scale-Cognitive-Japanese

⁶Logical memory II: Logical Memory II of the Wechsler Memory Revised

⁷ACE-R: the Addenbrooke's Cognitive Examination Revised (ACE-R)

Results

Patient's characteristics

There were no significant differences in age at examination, sex, and education levels between AD and HC. However, significant differences in MMSE, ADAS-cog-j,

logical memory II, and ACE-R scores were found between AD and HC (Table 1).

Relationship of SUVR of the posterior cingulate cortex using three reference regions

The relationship between SUVR_cerebellar cortex and SUVR_pons, and that between SUVR_cerebellar cortex and SUVR_corpus callosum, are shown in Figs. 2 and 3, respectively. Figure 2a shows high correlation between SUVR_cerebellar cortex and SUVR_pons (Spearman's rank correlation coefficient = 0.773). Using the regression equation, $SUVR_pons = 0.626 \times SUVR_cerebellar\ cortex - 0.0766$. Figure 2b shows the Bland–Altman plot between SUVR_cerebellar cortex and SUVR_pons. There were fixed bias (Mann–Whitney U test, $p < 0.01$) and proportional bias (Spearman's rank correlation coefficient = 0.630. Fixed bias was 0.636 (95% confidence intervals [CI] 0.590–0.681); SUVR_pons was lower than SUVR_cerebellar cortex in the same patient.

Similarly, Fig. 3a shows a high correlation between SUVR_cerebellar cortex and SUVR_corpus callosum (Spearman's rank correlation coefficient = 0.714). Using the regression equation, $SUVR_corpus\ callosum = 0.602 \times SUVR_cerebellar\ cortex + 0.098$. Figure 3b shows the Bland–Altman plot between SUVR_cerebellar cortex and SUVR_corpus callosum. There were fixed bias (Mann–Whitney U test, $p < 0.01$) and proportional bias (Spearman's rank correlation coefficient = 0.796. Fixed bias was 0.499 (95% CI 0.453–0.545); SUVR_corpus callosum was also lower than SUVR_cerebellar cortex in the same patient.

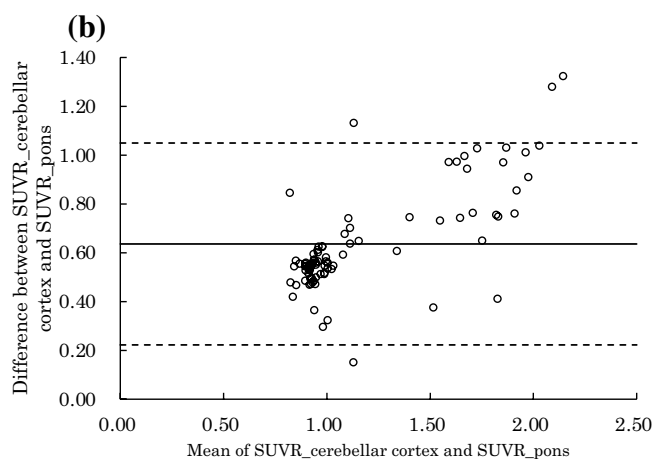
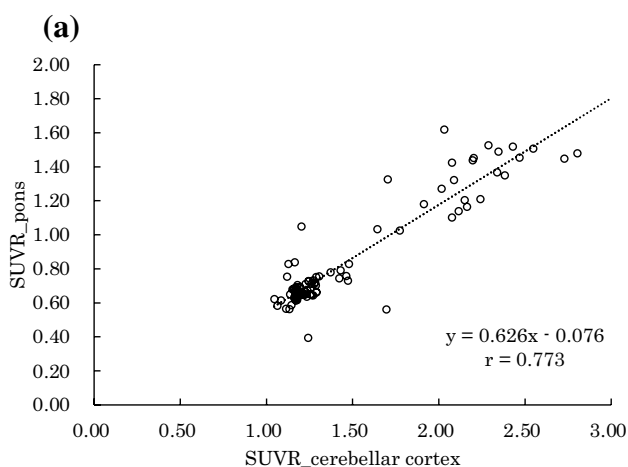


Fig. 2 **a** Shows the relationship between SUVR_cerebellar cortex and SUVR_pons (Spearman's rank correlation coefficient=0.773). Using the regression equation: $SUVR_pons = 0.626 \times SUVR_cerebellar\ cortex - 0.0766$. **b** Shows the Bland–Altman plot between SUVR_

cerebellar cortex and SUVR_pons. There were fixed (Mann–Whitney U test, $p < 0.001$) and proportional (Spearman's rank correlation coefficient=0.630) biases. Fixed bias was 0.636 (95% confidence intervals [CI] 0.590–0.681)

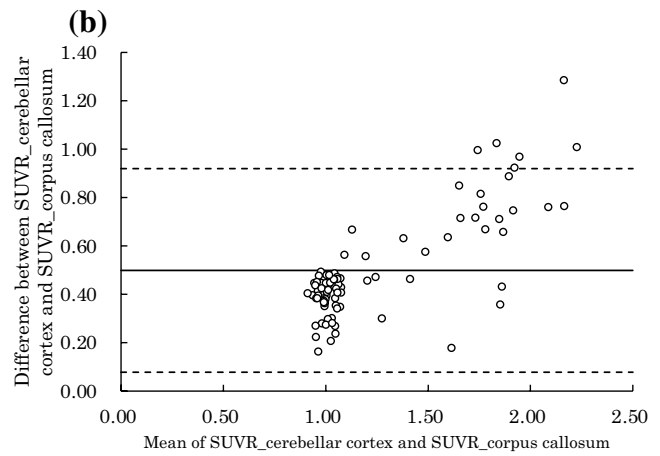
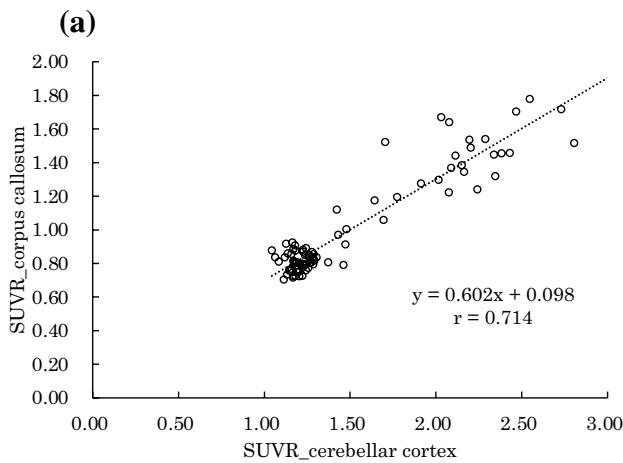


Fig. 3 **a** Shows the relationship between SUVR_cerebellar cortex and SUVR_corpus callosum (Spearman's rank correlation coefficient=0.714). Using the regression equation: $SUVR_corpus\ callosum = 0.602 \times SUVR_cerebellar\ cortex + 0.098$. **b** Shows the Bland–

Altman plot between SUVR_cerebellar cortex and SUVR_corpus callosum. There were fixed (Mann–Whitney U test, $p < 0.001$) and proportional (Spearman's rank correlation coefficient=0.796) biases. Fixed bias was 0.499 (CI 0.453–0.545)

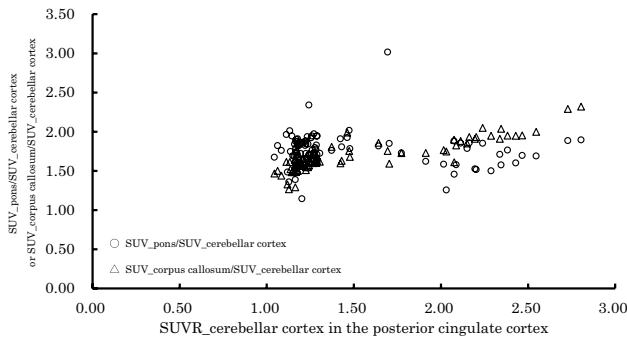


Fig. 4 The relationship of SUVR_cerebellar cortex in the posterior cingulate cortex with SUVR_pons/SUVR_cerebellar cortex and SUVR_corpus callosum/SUVR_cerebellar cortex. The SUVR_cerebellar cortex in the posterior cingulate cortex changed; however, the values of SUVR_pons/SUVR_cerebellar cortex and SUVR_corpus callosum/SUVR_cerebellar cortex are nearly constant between 1.5 and 2.0. That is, the values of SUVR_pons and SUVR_corpus callosum are approximately 1.5–2.0 times the value of SUVR_cerebellar cortex

The relationship of SUVR_cerebellar cortex in the posterior cingulate cortex with SUVR_pons/SUVR_cerebellar cortex and SUVR_corpus callosum/SUVR_cerebellar cortex

Figure 4 shows The relationship of SUVR_cerebellar cortex in the posterior cingulate cortex with SUVR_pons/SUVR_cerebellar cortex and SUVR_corpus callosum/SUVR_cerebellar cortex. This figure indicates that the changes in the values of SUVR_cerebellar cortex in the posterior cingulate cortex; however, the values of SUVR_pons/SUVR_cerebellar cortex and SUVR_corpus callosum/SUVR_cerebellar cortex were nearly constant between 1.5 and 2.0. That is, the values of

Table 2 The results of SUVR calculated using SUVmean

	Sensitivity	Specificity	Cut-off
Cerebellar cortex	100% (23/23)	100% (63/63)	1.694
Pons	100% (23/23)	96.8% (61/63)	0.839
Corpus callosum	100% (23/23)	100% (63/63)	1.177

In this study, all AD were PiB positive. They were assessed as “PiB positive” if the SUVRs, calculated with the cerebellar cortex as a reference region, were > 1.5. Therefore, the sensitivity and specificity were 100% when the cerebellar cortex was used as a reference region. The sensitivity was 100%, and the specificity was 96.8% when the pons was used as a reference region. When the corpus callosum was used as a reference region, both the sensitivity and specificity were 100%

SUVR_pons and SUVR_corpus callosum are approximately 1.5–2.0 times the value of SUVR_cerebellar cortex.

Comparison of diagnostic performance due to changes in the reference area

Table 2 and Fig. 5 show the results of ROC analysis when the pons and corpus callosum were used as the reference region. In this report, all AD were assessed as PiB positive. AD was assessed as PiB positive if the SUVRs, calculated using the cerebellar cortex as the reference region, were larger than 1.5. Accordingly, sensitivity and specificity were both 100% when the cerebellar cortex was used as the reference region. When the pons was used as the reference region, sensitivity was 100%, and specificity was 96.8%. When the corpus callosum was used as the reference region, sensitivity and specificity were both 100%.

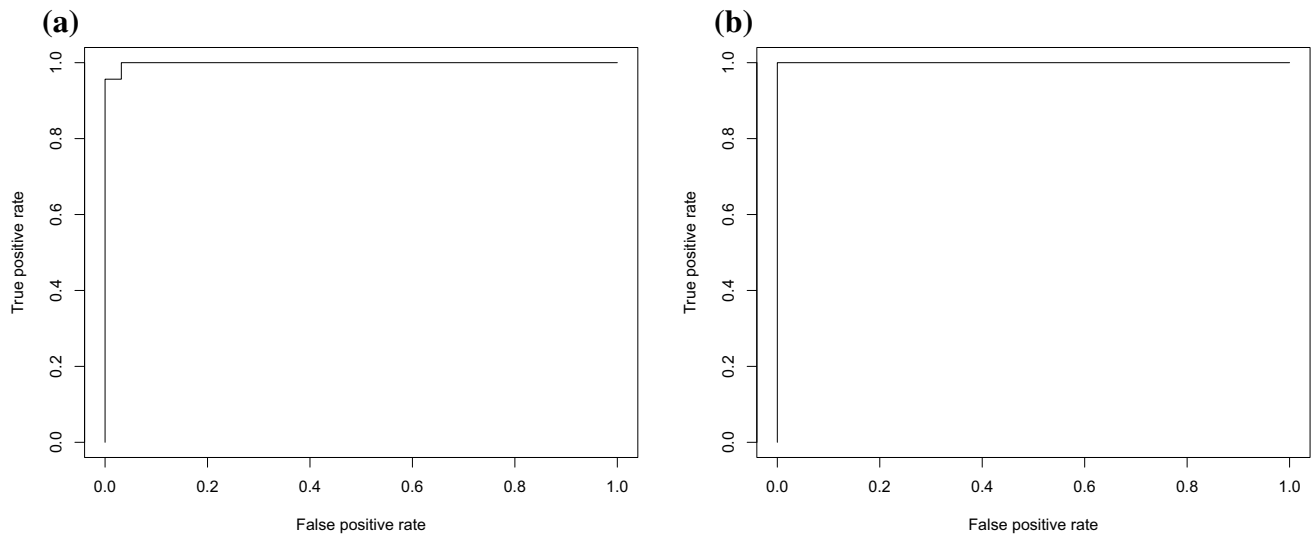


Fig. 5 Results of ROC analysis. **a** Shows the result of ROC analysis when the pons was used as the reference region. **b** Shows the result of ROC analysis when the corpus callosum was used as the reference region. When the pons was used as the reference region, sensitivity

was 100%; however, specificity was 96.8%. When the corpus callosum was used as the reference region, sensitivity and specificity were both 100%

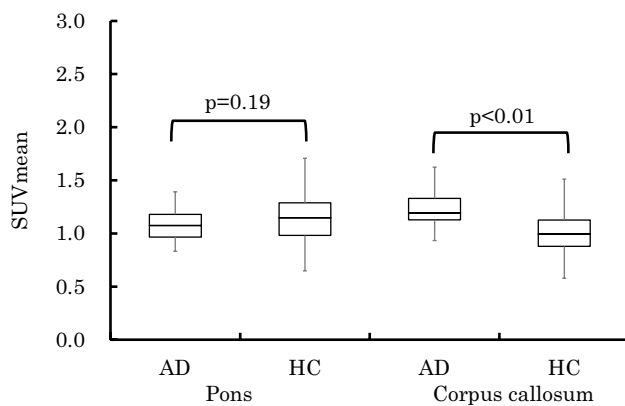


Fig. 6 Results of reference regions (SUVmean). There was no significant difference between Alzheimer's disease (AD) and healthy controls (HCs) in the cerebellar cortex and pons. However, there was a significant difference between AD and HCs in the corpus callosum

Comparison of ^{11}C -PiB accumulation between AD and HC

A comparison of ^{11}C -PiB accumulation between AD and HC in the reference regions is shown in Fig. 6. Mann–Whitney U test revealed that there was no significant difference between AD and HC in the pons ($p = 0.25$). However, there was a significant difference between AD and HC in the corpus callosum ($p < 0.01$).

Discussion

Our data suggested that SUV_{pons} and SUV_{corpus callosum} were highly correlated with SUV_{cerebellar cortex}. When the pons and corpus callosum were used as the reference region, sensitivity and specificity were both high. Therefore, both the pons and corpus callosum might be valid as reference regions for the quantitative evaluation of brain PET using ^{11}C -PiB. However, there were fixed and proportional biases when both the pons and corpus callosum were used as reference regions (Figs. 2, 3). Figure 4 shows that the values of SUV_{pons} and SUV_{corpus callosum} were nearly constant and are approximately 1.5–2.0 times higher than those of SUV_{cerebellar cortex} even when the value of SUV_{cerebellar cortex} in the posterior cingulate cortex was changed. This is the cause of the systematic error. Therefore, the SUV_R value varied depending on the reference region. It is necessary to use the regression equations that were used to perform the measurements in this study to evaluate the SUV_R value as well as that of the SUV_{cerebellar cortex}.

When the pons was used as the reference region, the specificity was only 96.8% (Fig. 5, Table 2). Edison et al. reported that, due to A β deposition in the cerebellar cortex, some AD show no significant differences with HC in cerebral cortical binding using the cerebellar cortex as a reference region, but higher ^{11}C -PiB binding in the cerebral and cerebellar cortices was revealed when the pons was used as a reference region [13]. In addition, Yokoi et al. reported that there may have been cases misevaluated

as PiB negative when they were PiB positive because of A β deposition in the cerebellar cortex.

Although there was no significant difference in the value of SUV between AD and HC in the pons, there was a significant difference in the corpus callosum ($p < 0.01$) (Fig. 6). The SUVR in AD may be underestimated when the corpus callosum was used as the reference region.

In this study, when the pons and corpus callosum were used as the reference region, SUVR_pons and SUVR_corpus callosum had a high correlation with SUVR_cerebellar cortex. In addition, it was found that even when the pons and corpus callosum are used as reference regions, AD and HC can be discriminated in the same manner as when the cerebellar cortex is used. For these reasons, the pons and corpus callosum are also considered to be valid reference regions for the quantitative evaluation of brain PET in AD patients, using ^{11}C -PiB. Therefore, when SUVR cannot be calculated accurately because of A β deposition or lesions in the cerebellar cortex, the pons and corpus callosum can be considered valid reference regions.

Moreover, in this study, ^{11}C -PiB PET and T1-weighted volumetric MR images were used for quantitative analysis. The T1-weighted MR images were often required to set the ROIs and obtain the SUVR. However, the acquisition of MR images had certain limitations. The acquisition time for the volumetric MR images was approximately 10 min. Patients with metal implants or pacemakers were not eligible for MR scanning. Furthermore, claustrophobic patients had to be excluded. In addition, the software required for setting the ROIs and obtaining SUVR automatically is expensive. An advantage of using the pons and corpus callosum as the reference region is that since their anatomical structures are less complicated than that of the cerebellar cortex, it is possible to set the ROI easily. In particular, using the pons and corpus callosum as the reference region is beneficial when setting the ROI manually.

This study had a few limitations. We did not include subjects whose SUVR could not be calculated accurately due to A β deposition in the cerebellar cortex or cerebellar lesions. In future studies, it would be necessary to study subjects in whom A β is already deposited in their cerebellar cortex and in patients with cerebellar lesions. We performed the Bland–Altman analysis to compare between SUVR_cerebellar cortex and both SUVR_pons and SUVR_corpus callosum resulting in systematic errors. It is considered that after recalibrating SUVR_pons and SUVR_corpus callosum to set them on the same scale as SUVR_cerebellar cortex would allow for a more sophisticated Bland Altman analysis [25]. In addition, the corpus callosum may have been affected by the partial volume effect because it has a thin structure and is close to the cerebral cortex. The corpus callosum is adjacent to the posterior cingulate cortex. Assuming that the full width at half maximum (FWHM) of the PET is

10 mm, the SUV_{mean} value of the corpus callosum in AD may be overestimated due to the spill over of PiB accumulated in the posterior cingulate cortex. On the other hand, the pons is about 5 cm away from the posterior cingulate cortex. Because it is five times farther away than FWHM, it may not be affected by the spill over of PiB accumulated in the posterior cingulate cortex. It is necessary to examine to what extent the corpus callosum is affected by the partial volume effect due to the spill over from each region in the cerebral cortex.

Conclusion

We examined the validity of using the pons and corpus callosum as reference regions for the quantitative evaluation of brain PET using ^{11}C -PiB, with reference to the cerebellar cortex as the reference region. Our data suggested that SUVR_pons and SUVR_corpus callosum were highly correlated with SUVR_cerebellar cortex. Furthermore, the sensitivity and specificity were high when either the pons or the corpus callosum was used as the reference region. Therefore, the pons and corpus callosum might be valid reference regions.

Acknowledgements We thank Editage (www.editage.com) for English language editing.

Funding None.

Data availability The data that support the findings of this study are available from the corresponding author, K.K., upon reasonable request.

Declarations

Conflict of interest The authors declare no conflicts of interest, financial or otherwise.

Open Access This article is licensed under a Creative Commons Attribution 4.0 International License, which permits use, sharing, adaptation, distribution and reproduction in any medium or format, as long as you give appropriate credit to the original author(s) and the source, provide a link to the Creative Commons licence, and indicate if changes were made. The images or other third party material in this article are included in the article's Creative Commons licence, unless indicated otherwise in a credit line to the material. If material is not included in the article's Creative Commons licence and your intended use is not permitted by statutory regulation or exceeds the permitted use, you will need to obtain permission directly from the copyright holder. To view a copy of this licence, visit <http://creativecommons.org/licenses/by/4.0/>.


References

- Okamura N, Harada R, Furukawa K, Furumoto S, Tago T, Yanai K, et al. Advances in the development of tau PET radiotracers and their clinical applications. *Ageing Res Rev.* 2016;30:107–13.
- Mathis CA, Wang Y, Holt DP, Huang GF, Debnath ML, Klunk WE. Synthesis and evaluation of ^{11}C -labeled 6-substituted

- 2-arylbenzothiazoles as amyloid imaging agents. *J Med Chem.* 2003;46:2740–54.
3. Camus V, Payoux P, Barré L, Desgranges B, Voisin T, Tauber C, et al. Using PET with ¹⁸F-AV-45 (florbetapir) to quantify brain amyloid load in a clinical environment. *Eur J Nucl Med Mol Imaging.* 2012;39:621–31.
 4. Sevigny J, Chiao P, Bussiére T, Weinreb PH, Williams L, Maier M, et al. The antibody aducanumab reduces A β plaques in Alzheimer's disease. *Nature.* 2016;537:50–6.
 5. Ferrero J, Williams L, Stella H, Leitermann K, Mikulskis A, O'Gorman J, et al. First-in-human, double-blind, placebo-controlled, single-dose escalation study of aducanumab (BIIB037) in mild-to-moderate Alzheimer's disease. *Alzheimers Dement (N Y).* 2016;2:169–76.
 6. Klunk WE, Price JC, Mathis CA, Tsopelas ND, Lopresti BJ, Ziolkowski SK, et al. Amyloid deposition begins in the striatum of presenilin-1 mutation carriers from two unrelated pedigrees. *J Neurosci.* 2007;27:6174–84.
 7. Chen K, Roontiva A, Thiyyagura P, Lee W, Liu X, Ayutyanont N, et al. Improved power for characterizing longitudinal amyloid- β PET changes and evaluating amyloid-modifying treatments with a cerebral white matter reference region. *J Nucl Med.* 2015;56:560–6.
 8. Okamoto K, Amari M, Ikeda M, Fukuda T, Suzuki K, Takatama M. A comparison of cerebral amyloid angiopathy in the cerebellum and CAA-positive occipital lobe of 60 brains from routine autopsies. *Neuropathology.* 2022;42:483–7.
 9. Takahashi Y, Oguchi K, Mochizuki Y, Takasone K, Ezawa N, Matsushima A. Distribution and progression of cerebral amyloid angiopathy in early-onset V30M (p.V50M) hereditary ATTR amyloidosis. *Amyloid.* 2022;30:1–10.
 10. Macdonell RAL, Kalnins RM, Donnan GA. Cerebellar infarction: natural history, prognosis, and pathology. *Stroke.* 1987;18:849–55.
 11. Bogousslavsky J, Van Melle G, Regli F. The Lausanne Stroke Registry: analysis of 1,000 consecutive patients with first stroke. *Stroke.* 1988;19:1083–92.
 12. Sybert GW, Alford EC Jr. Cerebellar infarction. A clinicopathological study. *Arch Neurol.* 1975;32:357–63.
 13. Edison P, Hinz R, Ramlackhansingh A, Thomas J, Gelosa G, Archer HA, et al. Can target-to-pons ratio be used as a reliable method for the analysis of C-11 PIB brain scans? *Neuroimage.* 2012;60:1716–23.
 14. Folstein MF, Folstein SE, McHugh PR. "Mini-mental state". A practical method for grading the cognitive state of patients for the clinician. *J Psychiatr Res.* 1975;12:189–98.
 15. Mioshi E, Dawson K, Mitchell J, Arnold R, Hodges JR. The Addenbrooke's Cognitive Examination Revised (ACE-R): a brief cognitive test battery for dementia screening. *Int J Geriatr Psychiatry.* 2006;21:1078–85.
 16. Rosen WG, Mohs RC, Davis KL. A new rating scale for Alzheimer's disease. *Am J Psychiatry.* 1984;141:1356–64.
 17. Wechsler D. Manual for the Wechsler adult intelligence scale-revised. New York: The Psychological Corporation; 1981. p. 156.
 18. Hughes CP, Berg L, Danziger WL, Coben LA, Martin RL. A new clinical scale for the staging of dementia. *Br J Psychiatry.* 1982;140:566–72.
 19. Morris JC. The Clinical Dementia Rating (CDR): current version and scoring rules. *Neurology.* 1993;43:2412–4.
 20. Yokoi T, Watanabe H, Yamaguchi H, Bagarinao E, Masuda M, Imai K, et al. Involvement of the precuneus/posterior cingulate cortex is significant for the development of Alzheimer's disease: a PET (THK5351, PiB) and Resting fMRI Study. *Front Aging Neurosci.* 2018;5(10):304.
 21. Hammers A, Allom R, Koeppe MJ, Free SL, Myers R, Lemieux L, et al. Three-dimensional maximum probability atlas of the human brain, with particular reference to the temporal lobe. *Hum Brain Mapp.* 2003;19:224–47.
 22. Gousias IS, Rueckert D, Heckemann RA, Dyet LE, Boardman JP, Edwards AD, et al. Automatic segmentation of brain MRIs of 2-year-olds into 83 regions of interest. *Neuroimage.* 2008;40:672–84.
 23. Edison P, Archer HA, Hinz R, Hammers A, Pavese N, Tai YF, et al. Amyloid, hypometabolism, and cognition in Alzheimer disease: an [¹¹C]PIB and [¹⁸F]FDG PET study. *Neurology.* 2007;68:501–8.
 24. Koivunen J, Scheinin N, Virta JR, Aalto S, Vahlberg T, Någren K, et al. Amyloid PET imaging in patients with mild cognitive impairment: a 2-year follow-up study. *Neurology.* 2011;76:1085–90.
 25. Taffé P. When can the Bland & Altman limits of agreement method be used and when it should not be used. *J Clin Epidemiol.* 2021;137:176–81.

Publisher's Note Springer Nature remains neutral with regard to jurisdictional claims in published maps and institutional affiliations.

Authors and Affiliations

Tomohiro Tada¹ · Kazuhiro Hara² · Naotoshi Fujita¹ · Yoshinori Ito³ · Hiroshi Yamaguchi⁴ · Reiko Ohdake⁵ · Kazuya Kawabata^{2,6} · Aya Ogura² · Toshiyasu Kato^{2,7} · Takamasa Yokoi⁸ · Michihito Masuda^{2,9} · Shinji Abe¹ · Shinichi Miyao¹⁰ · Shinji Naganawa¹¹ · Masahisa Katsuno^{2,12} · Hirohisa Watanabe⁵ · Gen Sobue¹³ · Katsuhiko Kato¹⁴ 

¹ Department of Radiological Technology, Nagoya University Hospital, 65 Tsurumai-Cho, Showa-Ku, Nagoya 466-8560, Japan

² Department of Neurology, Nagoya University Graduate School of Medicine, 65 Tsurumai-Cho, Showa-Ku, Nagoya 466-8550, Japan

³ Department of Radiological and Medical Laboratory Sciences, Nagoya University Graduate School of Medicine, 1-1-20 Daiko-Minami, Higashi-Ku, Nagoya 461-8673, Japan

⁴ Nagoya University Radioisotope Research Center Medical Branch, 65 Tsurumai-Cho, Showa-Ku, Nagoya 466-8550, Japan

⁵ Department of Neurology, Fujita Health University School of Medicine, 1-98 Dengakugakubo, Kutsukake-Cho, Toyoake, Aichi 470-1192, Japan

⁶ Department of Neurology, Medical University of Innsbruck, Innrain 52, 6020 Innsbruck, Austria

- ⁷ Department of Neurology, Anjo Kosei Hospital, 28 Higashihirokute Anjo-Cho, Anjo 446-8602, Japan
- ⁸ Department of Neurology, Toyohashi Municipal Hospital, 50 Hachikennishi, Aotake-Cho, Toyohashi 441-8570, Japan
- ⁹ Department of Neurology, Okazaki City Hospital, 1-3 Gosyoai, Kouryuji-Cho, Okazaki 444-8553, Japan
- ¹⁰ Department of Neurology, Meitetsu Hospital, 2-26-11 Sakou, Nishiku, Nagoya, Japan
- ¹¹ Department of Radiology, Nagoya University Graduate School of Medicine, 65 Tsurumai-Cho, Showa-Ku, Nagoya 466-8560, Japan
- ¹² Department of Clinical Research Education, Nagoya University Graduate School of Medicine, 65 Tsurumai-Cho, Showa-Ku, Nagoya 466-8560, Japan
- ¹³ Aichi Medical University, 1-1 Yazakokarimata, Nagakute, Japan
- ¹⁴ Functional Medical Imaging, Biomedical Imaging Sciences, Division of Advanced Information Health Sciences, Department of Integrated Health Sciences, Nagoya University Graduate School of Medicine, 1-1-20 Daiko-Minami, Higashi-Ku, Nagoya 461-8673, Japan